Liquid Ammonia injection on single hole injector: effect of initial conditions on flash boiling process

Anthony Desclaux, Ronan Pelé, Camille Hespel, Christine Mounaïm-Rousselle

Liquid Ammonia injection on single hole injector: effect of initial conditions on flash boiling process

A. Desclaux, R. Pelé, C. Hespel*, C. Mounaïm-Rousselle
Université d'Orléans, INSA-CVL, PRISME, EA 4229, F45072 Orléans, France
*Corresponding author: camille.hespel@univ-orleans.fr

Abstract
Due to its low boiling point, liquid ammonia is very sensitive to flash boiling phenomenon when the injection into a chamber is done in an ambient pressure below the saturation pressure. The characteristics of superheated ammonia spray on a well-established single-hole injector have been experimentally investigated. Different fuel temperatures and ambient densities are considered to cover a wide range of superheat degree. It was found that the spray geometry and morphology are very sensitive to the superheat degree: the angles near the injector and at half of the penetration length increase with the superheat degree. An opposite trend in air density and superheat degree on the spray penetration has been identified. Finally, the cooling effect due to the flash boiling process was characterized.

Introduction

Ammonia is more and more considered as an attractive carbon-free alternative fuel for transportation and power generation. Some studies have already been devoted to the injection of gaseous ammonia, while those using direct injection of liquid ammonia remain quite rare. Recently, the liquid injection of ammonia has been considered not only for internal combustion engines (ICE) [1, 2] but also gas turbines (GT) [3, 4]. For ICE, direct injection of liquid ammonia is preferred to control the in-cylinder air-fuel ratio, to optimize the thermal efficiency and limit the unburnt ammonia. Pelé et al. [2] indicated that optimized trade-off between unburnt NH_3 and NOx emissions can be reached as a function of direct liquid ammonia injection strategy in a single cylinder direct injection Spark ignition engine. For gas turbines, the injection of liquid ammonia induces a reduction of the cost and size compared to gaseous ammonia injection. Okafor et al. [4] investigated the combustion stability and emissions of liquid ammonia spray in a gas turbine combustor. They found that it is necessary to use preheated swirling air to enhance flame stability due to the strong cooling effect of liquid ammonia induced by the instantaneous spray flash-boiling and high latent heat of vaporization. They also concluded that the flash-boiling effect is crucial to stabilize ammonia combustion and must be considered in the design of internal engines and gas turbines.

Many studies have been devoted to the study of flash-boiling spray in the last few decades, as reviewed by Bar-Kohany et al. [5]. Flash boiling occurs when fuel is injected into a chamber with an ambient (P_{amb}) pressure below the saturation pressure (P_{sat}). The rapid reduction of pressure during the injection process causes the superheat of the liquid jet. The formation of flash boiling comprises three stages: bubble nucleation, bubble growth and the two-phase flow. It can occur outside and inside the injector, where the bubbles grow, and the two-phase flow is ejected. Although, flash-boiling process depends on several factors such as fuel temperature, pressure, injector geometry and hole number. The rate of bubble formed during this process is commonly related to the super heat degree parameter, R_p, defined in equation (1).

$$R_p = \frac{P_{sat}\left(T_f\right)}{P_{amb}} \quad (1)$$

Where $P_{sat}(T_f)$ is the saturation pressure at the liquid fuel temperature.

Based on the characteristics of the inner flow, the spray atomization and evaporation, the flashing liquid jet regimes can be classified into three main categories named the initial flashing, transitional-flashing and flare-flashing regimes. Transitions between these regimes are determined mainly by the level of superheat, which sets nucleation regime and bubble growth rate, which are of major influence on the spray behaviour. Therefore, the superheat level is mainly quantified using R_p or via the Kitamura's criterion [6], expressed with the ratio between the sensible heat and the latent heat versus the Weber number of the vapor. In the case of liquid ammonia spray, Li et al. [7] found that the different flashing regions of superheated ammonia spray can be divided into the initial-flashing region ($1 < R_p \leq 2$), transitional-flashing region ($2 < R_p \leq 5$), and flare-flashing region ($R_p > 5$). Considering the aerodynamic interaction between the liquid fuel jet and the ambient air, the spray evolution process is commonly described using the spray tip penetration (S). For liquid ammonia, Pelé et al. [1] investigated the macroscopic characteristics of the spray injected from a 7 holes injector. A semi-empirical penetration model

was established during a fixed time range between 0.8-1.8 ms after the start of fuel injection and the penetration tip shows a $t^{0.619}$ dependence. Li et al. [7] investigated both micro-and macroscopic features of the jet injected from an in-house single hole injector. They found that ammonia spray penetration is divided into the flashing dominated stage, the transition stage and the quasi-steady stage according to other study [8] performed with high-pressure diesel fuel injector.

Due to its low boiling point, liquid ammonia is very sensitive to flash boiling, especially under relevant conditions for ICEs and GTs, where liquid fuel is injected from the spray nozzle into a chamber with an ambient pressure below the saturation pressure. However, the characteristics of the superheated ammonia spray are not fully understood due to the combined effects of flash boiling in the nozzle as well as in the near field and strong aerodynamic interactions during its penetration process. In this experimental study, the characteristics of superheated ammonia spray on a single hole injector, based on Spray G injector (https://ecn.sandia.gov/gasoline-spray-combustion) were investigated in a constant volume chamber. Schlieren technique was adopted to measure both liquid and liquid/vapor ammonia spray and the temperature along the spray was achieved using thermocouples.

Experimental means and methods

Experimental apparatus and techniques

The experimental setup (Fig.1) consists of a stainless-steel spherical vessel of 4.2 L. To allow optical access, the vessel is equipped with four quartz windows. In this setup, the pressure is adjustable until 10 bar by air filling system and the temperature is controlled up to 200 °C by wall heating resistances. The injector is mounted on the upper part of the vessel. Liquid ammonia is pressurized up to 120 bar in a tank by means of pressurized helium. The injection duration is controlled with an injector power driver (EFS 8427) and the temperature is set using a temperature control system connected to a liquid jacket surrounding the injector to maintain the fuel temperature at a desired temperature between -10°C to 50°C. All these parameters are measured using type K thermocouples. The injection pressure was fixed at 70 bar, controlled via a pressure sensor Keller 0-300 bar. Finally, the fuel injection is triggered with imaging and recording system using NI cRIO 9024.

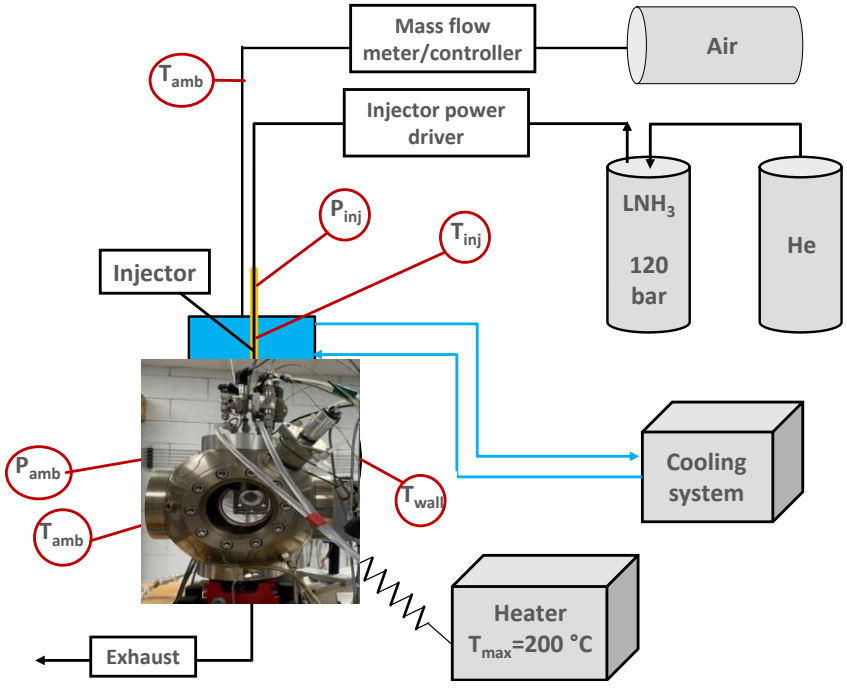

Figure 1. Experimental set up.

The morphology of the spray, including both liquid and vapor phase is determined via a Schlieren set-up. This optical arrangement is composed of a high-power light emitting diode (LED), a pair of concave mirrors, a lens with a focal of 200 mm and an adjustable pinhole. The resulting images are recorded by a high-speed camera Phantom V1611 with a maximum frame rate of 45 kHz. Frame size and the exposure time were respectively fixed to 5µs and 256 x 800 $pixel^2$. The cooling effect caused by the flash boiling process was measured using three 25 µm thermocouples type K arranged along the spray.

Experimental conditions

A single hole injector, labelled Spray M by ECN, with a hole diameter D_{inj} of 165 µm with an aspect ratio, hole length/D_{inj}, equal to 1.4 was used in this study. The superheat degree is represented by the pressure ratio, R_p. To investigate the liquid ammonia spray in a broad range of flash boiling conditions. For that, different combinations of ambient pressure and fuel temperature were considered, providing a R_p range from 0.59 to 19.24. Detailed specification and experimental conditions are summarized in Tab.1 and in Fig.2.

Table 1. Experimental conditions

Description (units)	Value
Injection duration (ms)	7
P_{inj} (bar)	70
T_f (°C)	-10 - 50
T_{amb} (°C)	28 ± 1.5
P_{amb} (bar)	1 - 7
ρ_{air} (kg/m^3)	1.12 - 8
R_p (-)	0.59 – 19.24

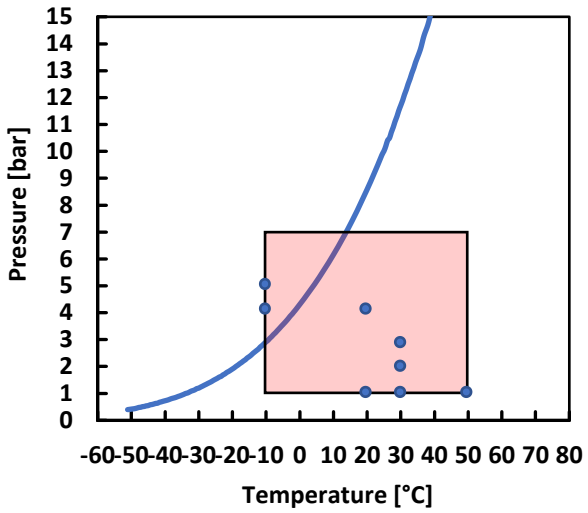

Figure 2. Liquid-vapor phase P-T diagram for NH_3.

Imaging and data processing method

The geometry of the spray was accurately determined using an in-house MATLAB image processing program. To obtain information about the spray development such as the penetration, the width and the angle of the spray, the raw images are processed using binarization procedure. The first thirteen images, without the spray, are used to generate an average background. After subtraction of this average background, the images are binarized using the Ostu threshold [9] to identify the edge of the liquid phase of the spray to determine the contour. The definition of the spray penetration and cone angle is demonstrated in Fig.3. The penetration (S) is defined as the vertical distance between the nozzle and the maximum point reached by the liquid spray and the cone angle (α) is defined as the value of the angle from the nozzle outlet to the half penetration of the spray as follow:

$$\alpha = 2arctan\left(\frac{A_{S/2}}{(S/2)^2}\right) \quad (2)$$

Where $A_{S/2}$ is the spray projected area at the half penetration (S/2).

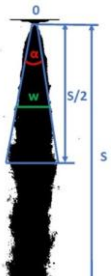

Figure 3. Definition of the spray penetration (S) and angle (α).

Results and discussion

In this section the characterization of the dynamics of the liquid ammonia spray is presented within a wide range of superheat degrees. All average values and standard variation bars shown through these results are obtained on 10 identical tests performed for each condition studied. First, the analyse of the morphology of the spray is presented. Then, the characteristics of the spray in terms of spray penetration and angle is studied. Finally, the cooling effect caused by the flash boiling process is presented.

Spray Morphology

Ammonia spray snapshots are presented in Fig.4. for different conditions of R_p represented by blue symbols in Fig.2. For R_p <1, in Fig.4 (a) and (b), the flash boiling phenomenon does not occur. From R_p = 2.18 (Fig.4 (c)), the spray is slightly wider as the flash boiling occurs. As R_p increases, the spray expands and its appearance near the injector changes by an increase of the near-nose spray angle. For $3.85<R_p<8.85$, the width of the spray increases until reached a critical size for R_p > 8.85 (Fig.4 (f)). It can also be noticed that as a function of the superheat degree, a kind of a liquid tube near the nozzle outlet is more and more pronounced before the flaring of the spray. This phenomenon is not distinguishable for non-flashing conditions.

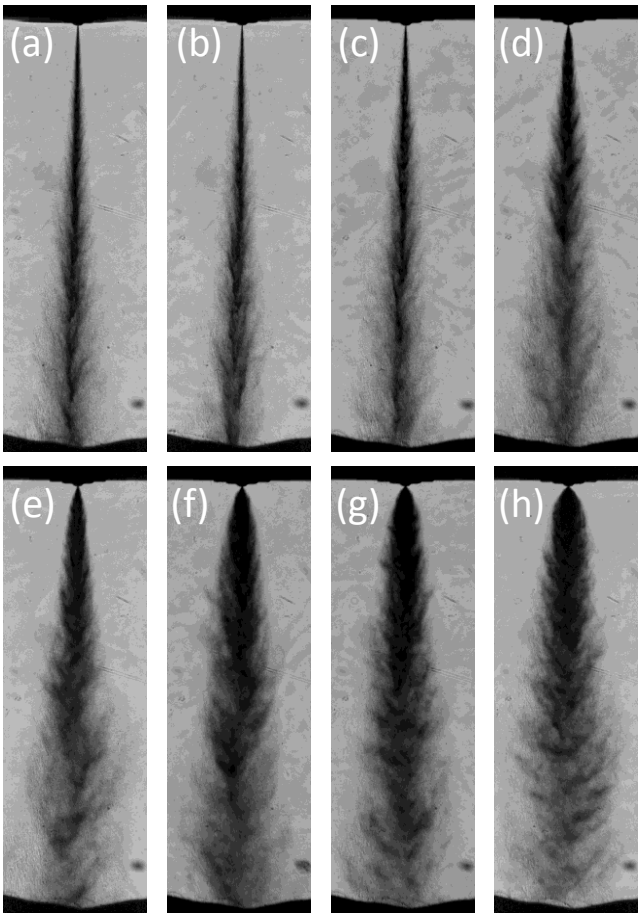

Figure 4. Morphological features of superheated ammonia spray: (a) R_p=0.59, T_f=-10°C - P_{amb}=5 bar ; (b) R_p=0.73, T_f=-10°C - P_{amb}=4 bar ; (c) R_p=2.18, T_f=20°C - P_{amb}=4 bar ; (d) R_p=3.85, T_f=30°C - P_{amb}=3 bar ; (e) R_p=5.72, T_f=30°C - P_{amb}=2 bar ; (f) R_p=8.85, T_f=20°C - P_{amb}=1 bar ; (g) R_p=11.37, T_f=30°C - P_{amb}=1 bar ; (h) R_p=19.24, T_f=50°C - P_{amb}=1 bar.

Spray characteristics

In this section, characteristics of the superheated ammonia spray, including the evolution of the spray penetration and angle determined for the half penetration are analysed. First, to analyse the influence of the superheat degree on the spray behaviour, the temporal evolution of the spray penetration is plotted for isobaric (P_{amb}=2 bar) and isothermal (T_f=-10°C) conditions respectively shown in Fig.5 (a) and (b). As one can see on Fig.5 (a), the spray penetration is similar for all fuel conditions for the first time after the beginning of the injection until to 0.2 ms. Then the spray penetration decreases as a function of the superheat degree level. In Fig.5 (b), the spray penetration is presented for pressure conditions ranging from 1 to 5 bar, corresponding to a range of air density of 1.1 to 5.8 kg.m^{-3} and a range of R_p = 0.59 – 3.01. As expected, for pressure conditions ranging from 2 to 5 bar, the spray penetration decreases with the increases of the air density. On the contrary, for the lowest pressure condition, corresponding to an air density of 1.1 kg.m^{-3} and a superheat degree of 3.01, the spray penetration is lower. These results show an opposite trend of air density and superheat degree on the spray penetration and a greater influence of superheated degree than the air density from R_p value above 3.

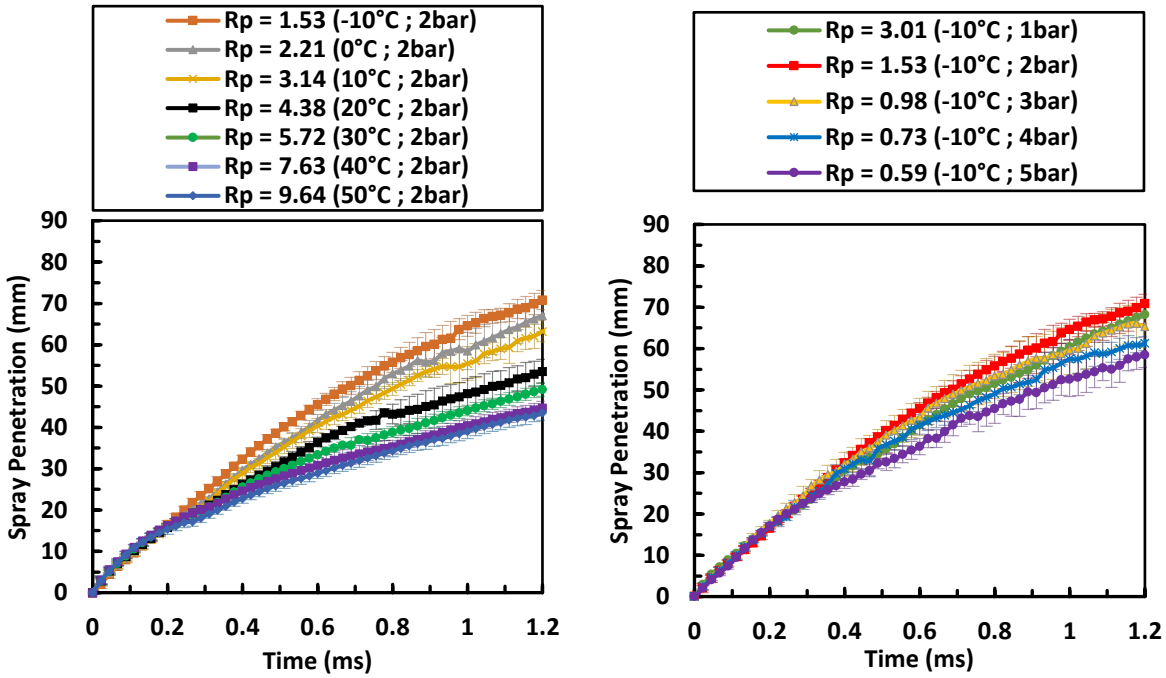

Figure 5. Effect of R_p on liquid penetration of ammonia spray for (a) isobaric conditions P_{amb} = 2 bar and (b) isothermal conditions T_f = -10 °C

To better understand the spray penetration behaviour, Fig.6 shows the effect of R_p, depending on ρair, on the spray length penetration at the same given time of 0.8 ms, for all tested conditions. As one can see, the penetration length increases from R_p=0.59 to R_p=1.5 with the decreases of the air density. Then the penetration decreases with the superheat degree increase for all air density conditions and tends to a constant value for largest values of R_p. The influence of ρ_{air} on spray penetration is weak for 1.5<R_p<4, then increases with the increases of R_p. In comparison with non-flashing spray, one would have expected a decrease in spray penetration as a function of ρ_{air} over the full range of tested conditions. Nevertheless, the increase of superheat degree dominates this trend.

In Fig.7, the evolution of the mean spray angle, as usually defined for an established spray, at the half-penetration is plotted versus the superheat degree and depending on ρ_{air}, for all tested conditions. First, depending on R_p, globally the spray angle increases over the full range of tested conditions until reach a plateau, constant for R_p > 8, without any effect of air density. But for smaller R_p, i. e. below 3, the air density has a significant effect even if no evident trend can be suggested. As for the spray penetration, the superheat degree and so the flash boiling effect dominates the mean spray angle evolution.

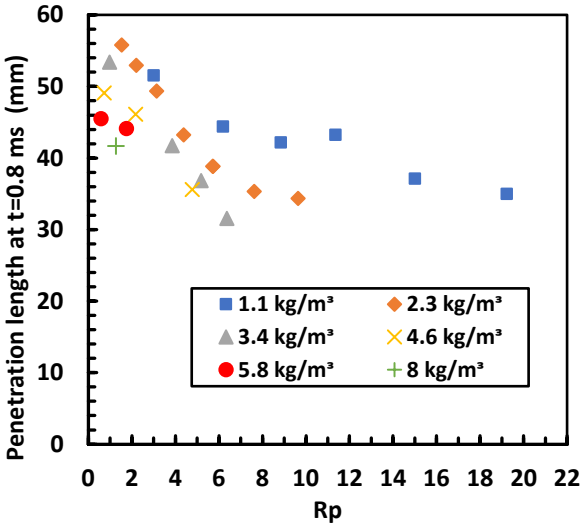

Figure 6. Evolution of the spray penetration length at 0.8 m/s after beginning of injection as a function of the superheat degree for all tested conditions.

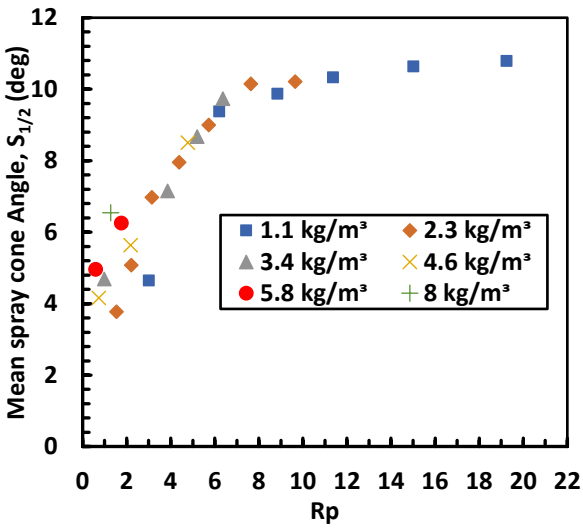

Figure 7. Evolution of the mean spray angle for the half-penetration versus the superheat degree.

Fig.8 compares the effect of R_p on the fitted time exponent of the first stage of the injection (0.3 ms) within all tested conditions. In this stage, the penetration evolution is not only related to the needle lift but also the bubble explosion due to the flash boiling at the nozzle exit. The spray momentum in the axial direction decreases as the increase of R_p, and the fitted time exponent gradually falls and stabilizes around 0.45 from R_p=10. Unlike the effect on the angle, a significant effect of the air density is observed for R_p>3.

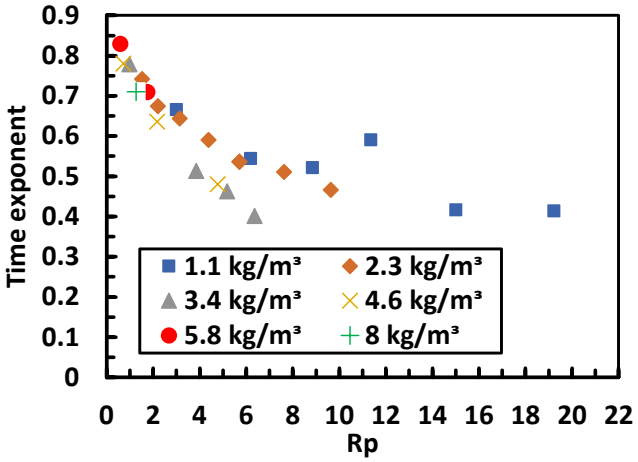

Figure 8. Effect of the superheat degree on the fitted time exponent for the first stage of the injection (0.3 ms).

Thus, comparing the results of the spray penetration and fitted time exponent with those obtained for mean spray angle, it can be concluded that the decrease of the vertical spray penetration is due to the increase of the lateral expansion the spray, which only depends on the superheat degree for R_p>4.
These results confirm that the flashing region of superheated ammonia is divided into three different regimes: the initial-flashing, the transitional flashing and the flare-flashing region. However, the influence of the air density on the spray characteristics shows that a classification based on R_p only is no longer valid and not sufficient.

Flash boiling cooling effect

In this section, the cooling effect caused by the flash boiling process due to the large latent heat vaporization is explored. For this purpose, temperature measurements by using a combination of three thermocouples, as shown in Fig. 9, have been performed. First, as an example, three different superheat degree values corresponding to R_p=0.89, 4.38 and 15.4 are presented (Fig.10 (a), (b) and (c)). Then, a complete exploration has been performed for R_p=15.4 condition for different lateral positions with a step of 0.7 mm. Finally, measurements of the spray temperature, made as close as possible to the spray for a large range of experimental conditions summarized in Table.2, are compared with that obtained by numerical simulation based on an equilibrium model of evaporation of a stationary drop developed by Pelé et al. [10]. This model consists in using the classical model with Spalding number of [11] and [12]. To consider instantaneous boiling, the model of [13] is used to study the evaporation of aqueous ammonia droplets. The heat transfer equation is implemented in the model and the initial radius of the droplet is fixed at 5µm.

Figure 9. Visualization of the thermocouple location.

Fig.10 compares the evolution of the spray temperature versus the time for the three superheat degree conditions. The temperature obtained by all thermocouples reaches the minimum value of -60°C for R_p=15.4 and 4.38, corresponding to flash boiling conditions, while for R_p=0.89, the minimum tis around -40°C.

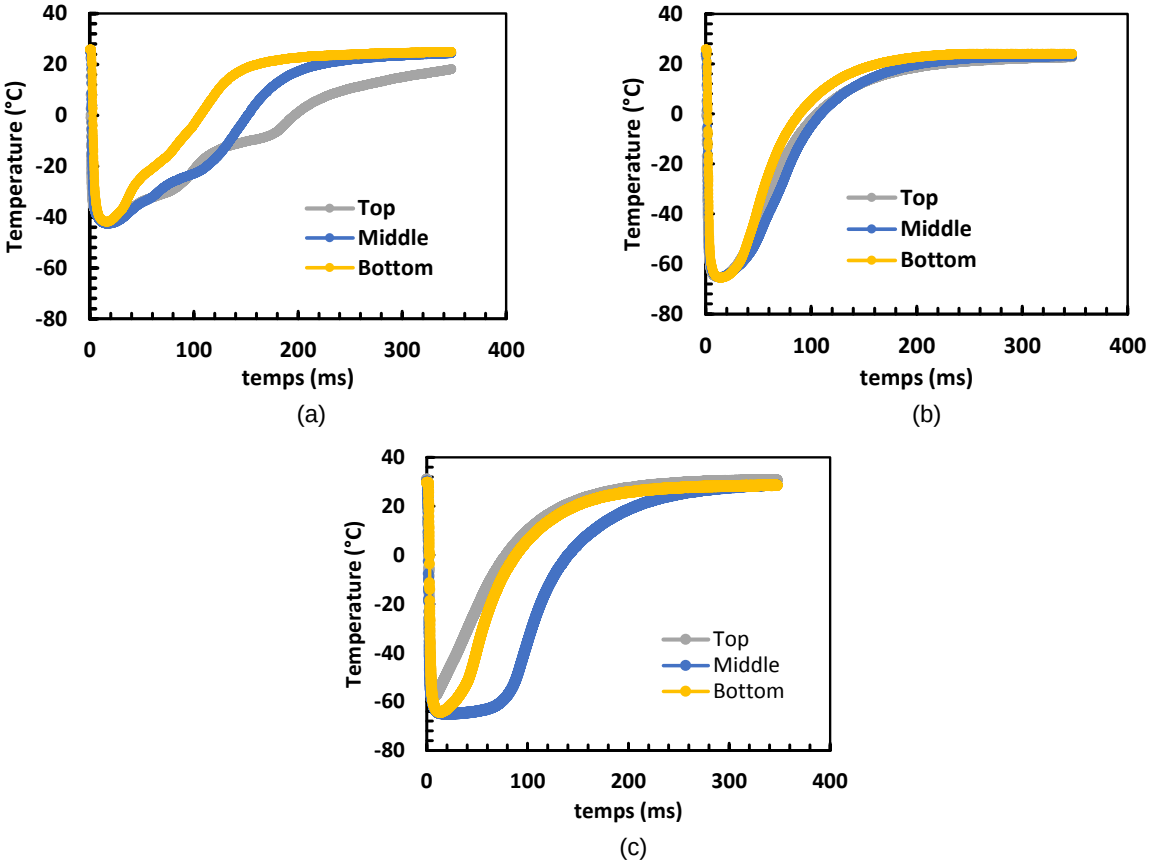

Figure 10. Temporal evolution of the spray temperature: (a) R_p=0.89, T_f=-10°C - P_{amb}=3 bar; (b) R_p=4.38, T_f=20°C - P_{amb}=2 bar; R_p=15.4, T_f=40°C - P_{amb}=1 bar.

Fig.11 presents the evolution of the temperature profile versus the lateral position measured via the three thermocouples for the superheat degree condition, R_p=15.4. As expected, the temperature increases by moving away from the spray axis, but the equilibrium temperature is reached at different x location as a function of the axial location, i.e. for the top thermocouple at x=5mm, for the middle and bottom thermocouples for x>10mm remains constant, with a temperature maintained around -60°C, over 2.5 mm This is due to the geometry of the spray and the presence of the vapor phase, caused by the flash boiling process, in the middle and at the end of the spray plume.

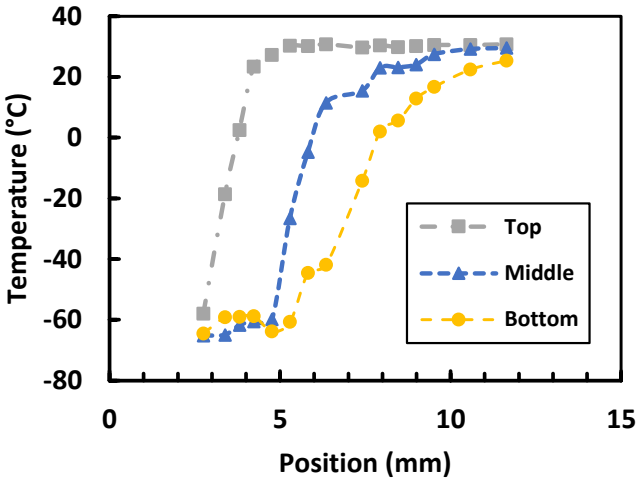

Figure 11. Evolution of the temperature profile versus the lateral positions for R_p=15.4, T_f=40°C and P_{amb}=1 bar.

Fig.12 shows the comparison between the evolution of the spray temperature obtained experimentally with thermocouples and that obtained by numerical simulation based on an equilibrium stationary drop evaporation model adapted to the flash boiling process [10]. Fig.12 (a) and (b) represent, respectively, the evolution of the spray temperature versus the superheat degree (R_p) and versus the ambient pressure (P_{amb}). These results show a very good agreement between the experimental measurements and the numerical model. Fig.12 (a) shows a non-monotonic evolution of the spray temperature as a function of R_p. Fig.12 (b) shows that the spray temperature increases with P_{amb}. From these results (Fig.12 (a) and (b)) and Table.2, it can be observed that the spray temperature depends mainly on the ambient pressure (P_{amb}) while the influence of the saturation pressure at the specific fuel temperature ($P_{sat}(T_f)$) is negligible. This analysis shows the influence of the evaporation process on the behaviour of the spray temperature evolution (Fig.12 (a)) as well as the penetration (Fig.6) and the spray plume expansion (Fig.4) versus of the superheat degree. Consequently, these results show that the use of an equilibrium evaporation model is viable to model the spray under flash boiling and non-flashing conditions and that the experimental measurement method using thermocouples is relevant. From results, a more in-depth analysis of these results, using experimental data and numerical simulation results, will be carried out in future work.

Table 2. Experimental conditions used to analyse the spray temperature.

Description (units)	Value									
Rp [-]	0.59	0.89	1.53	2.21	3.01	4.3	5.29	6.2	8.85	15.4
P_{amb} [bar]	5	7	2	2	1	1	3	1	1	1
T_f [°C]	-10	10	-10	0	-10	0	40	10	20	40
P_{sat}(Tf) [bar]	2.9	6.2	3	4.4	2.9	4.4	15.4	6.2	8.8	15.4

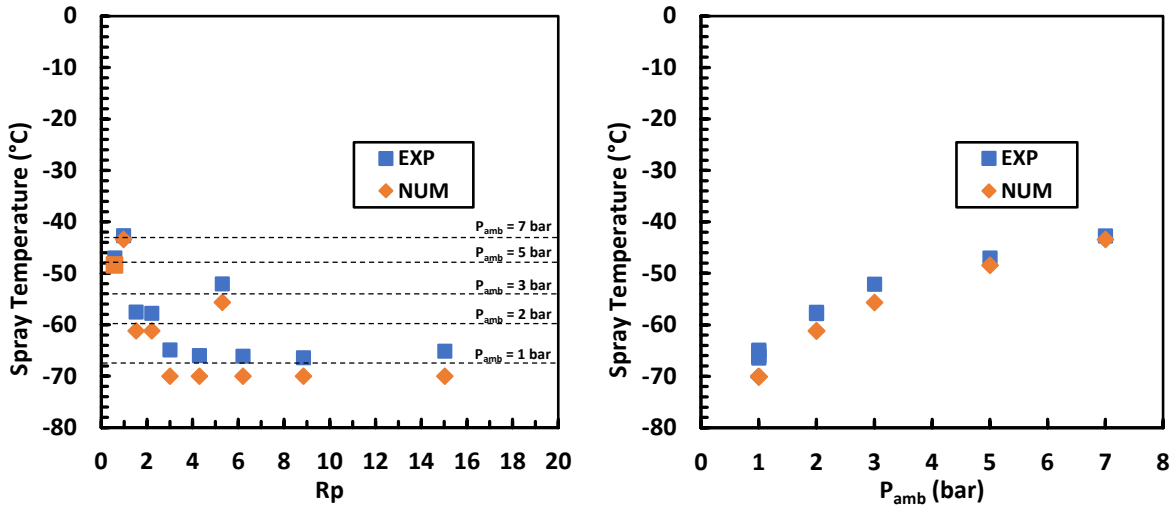

Figure 12. Evolution of spray temperature (a) versus the superheat degree and (b) versus the ambient pressure for R_p=0.59, T_f=-10°C - P_{amb}=5 bar ; R_p=0.89, T_f=10°C - P_{amb}=7 bar ; R_p=2.18, T_f=20°C - P_{amb}=4 bar ; R_p=3.01, T_f=-10°C - P_{amb}=1 bar ; R_p=4.3, T_f=0°C - P_{amb}=1 bar ; R_p=5.29, T_f=40°C - P_{amb}=3 bar ; R_p=6.2, T_f=10°C - P_{amb}=1 bar ; R_p=8.85, T_f=20°C - P_{amb}=1 bar ; R_p=15.04, T_f=40°C - P_{amb}=1 bar.

Conclusions

In this study, the characteristics of superheated ammonia spray have been investigated over broad range of experimental conditions. The spray morphology, angle, penetration and fitted time exponent have been determined. It was observed that the decrease of the vertical spray penetration is due to the increase of the lateral expansion of the spray, which only depends on the superheat degree. These results show a great influence of the superheat degree on the spray characteristics, compensated by an opposite effect of the air density. As shown by Li et al. [7], the flashing regions of superheated ammonia spray could be divided into 3 phases (initial-flashing, transitional-flashing and flare flashing regions). Nevertheless, the influence of the air density on the spray characteristics indicates that a classification depending only on R_p is no longer valid. In this case, the use of the Kitamura criterion [6], which considers the density of the air in its expression is more appropriate. Further work is then necessary to propose a modified correlation of the criterion adapted to liquid ammonia injection. Finally, the cooling effect due to the significant vaporization of latent heat was successfully obtained via thermocouple measurements and compared with a numerical simulation based on an equilibrium evaporation model for one droplet. The results show a very good agreement and highlights the use of an equilibrium evaporation model is viable to model the spray under flash boiling and non-flashing conditions and that the experimental measurement method using thermocouples is relevant. From results, a more in-depth analysis of these results, using experimental data and numerical simulation results, will be carried out in future work.

Acknowledgements

The work has been partially financed by ANR for the ADONIS Project ANR-22-HTCE-0001-02 call EIG CONCERT-Japan 2021. The content of this paper reflects only the author's view.

Nomenclature

P_{inj}	Injection pressure [bar]
P_{amb}	Ambient pressure [bar]
T_f	fuel temperature [K]
T_{amb}	Ambient temperature [K]
ρ_{air}	Air density [kg.m^{-3}]
R_p	Superheat degree [-]

References

[1] Pelé, R., Mounaïm-Rousselle, C., Bréquigny, P., Hespel, C., Bellettre, J. (2021). First study on ammonia spray characteristics with a current GDI engine injector. Fuels, 2(3), 253-271.

[2 Pelé, R., Brequigny, P.; Bellettre, J.; Mounaïm-Rousselle, C. (2023), Performances and pollutant emissions of spark ignition engine using direct injection for blends of ethanol/ammonia and pure ammonia, International Journal of Engine Research, accepted IJER-22-0314.R1

[3] Okafor, E. C., Yamashita, H., Hayakawa, A., Somarathne, K. K. A., Kudo, T., Tsujimura, T., Kobayashi, H. (2021). Flame stability and emissions characteristics of liquid ammonia spray co-fired with methane in a single stage swirl combustor. Fuel, 287, 119433.

[4] Okafor, E.C., Kurata, O., Yamashita, H., Inoue, T; Tsujimura, T., Iki, N., Hayakawa, A., Ito, S., Uchida, M., Kobayashi, H., (2021). Liquid ammonia spray combustion in two-stage micro gas turbine combustors at 0.25 MPa; Relevance of combustion enhancement to flame stability and NOx control, Applications in Energy and Combustion Science, 7, 100038.

[5] Bar-Kohany, T., Levy, M., (2016). State of the art review of flash-boiling atomization. Atomization Sprays, 26(12).

[6] Kitamura, Y., Morimitsu, H., Takahashi, T. (1986). Critical superheat for flashing of superheated liquid jets. Industrial & engineering chemistry fundamentals, 25(2), 206-211.

[7] Li, S., Li, T., Wang, N., Zhou, X., Chen, R., Yi, P. (2022). An investigation on near-field and far-field characteristics of superheated ammonia spray. Fuel,324, 124683.

[8] Li, T., Zhou, X., Wang, N., Wang, X., Chen, R., Li, S., (2022). A comparison between low- and high-pressure injection dual-fuel modes of diesel-pilot- ignition ammonia combustion engines. J Energy Inst, 102:362–73.

[9] Otsu, N. A, (1979). Threshold Selection Method from Gray-Level Histograms. IEEE Trans. Syst. Man Cybern. 9, 62–66.

[10] Pelé, R., Brequigny, P., Hespel, C., Bellettre, J., Mounaïm Rousselle, C., (2023). Spray Characteristics and Vaporization Process of Ammonia-Ethanol blends with a Current GDI Engine Injector ; ILASS, *under review.*

[11] Sazhin, S.S., Elwardany, A., Krutitskii, P.A., Castanet, G., Lemoine, F., Sazhina, E.M., Heikal, M.R., (2010). A simplified model for bi-component droplet heating and evaporation. Int. J. Heat Mass Transf. 53, 4495–4505.

[12] Ni, Z., Hespel, C., Han, K., Foucher, F., (2021). The non-ideal evaporation behaviors of ethanol/heptane droplets : Impact on diameter, temperature evolution and the light scattering by droplet at the rainbow angle; Int. J. Heat Mass Transf. 164

[13] T. Eldredge, M. Thomas, (2018). Investigation of the Evaporation Processes for Aqueous Ammonia and Aqueous Urea and Guidelines for Using Simplifying Assumptions. Am. Soc. Mech. Eng. Power Div. POWER 1, 1-7.